# ASSESSMENT OF THERMALLY INDUCED STRESS IN BIPV MODULES USING FEM SIMULATIONS

Andreas J. Beinert[1], Achour Mahfoudi[1], Frank Ensslen[1], Christof Erban[2], Pascal Romer[1]
[1]Fraunhofer Institute for Solar Energy Systems ISE, Heidenhofstraße 2, 79110 Freiburg, Germany
[2]SUNOVATION, Glanzstoffstraße 21, 63820 Elsenfeld, Germany
*Corresponding author:* Andreas J. Beinert | Phone: +49 (0)761 4588 5630 | E-mail: Andreas.Beinert@ise.fraunhofer.de

ABSTRACT: Environmental conditions like irradiation and temperature cause thermally induced stresses in building-integrated PV modules. This study investigates the influences of different design parameters and additionally environmental conditions on the thermally induced stresses within the glass of BIPV modules. A thermomechanical 3D FEM model of a glass-glass BIPV module in an example ventilated façade is used to perform parameter sensitivity studies. Among the investigated variations, partial shading has the strongest impact. All simulated variations result in maximum stresses above the design edge resistance of annealed glass. Therefore, the use of annealed glass is risky, while the design edge resistance of thermally toughened glass was not exceeded in any variation.
From the detailed 3D FEM model, a simplified 2D FEM model was derived for the purpose of a quick and easy estimation of the thermally induced stress.
The approach "Determination of thermomechanical resistance to partial shading" was proposed for discussion by the standardization committee responsible for revising EN 50583:2016.
Keywords: FEM simulation, Thermal stress, Digital prototyping,

## 1 INTRODUCTION

For the mechanical design of building-integrated PV modules (BIPV) in façades and roofs, the loads due to self-weight, wind and snow have been sufficiently well studied and are taken into account in engineering practice. However, these modules are also exposed to thermally induced loads from direct solar radiation. The standards and guidelines available to date, both at the German and the European level, contain only simplified information and specifications for calculating the thermally induced stresses. Within the scope of the research project with the acronym "Thermobruch" [1,2], building-integrated glass-glass PV modules, e.g. as components of a ventilated façade, are investigated by means of the finite element method (FEM) using long-term German meteorological data. The aim is to reduce or prevent the occurrence of thermally induced glass breakage by taking appropriate measures already in the planning phase by applying the developed simulation approaches.

## 2 METHOD

A 3D thermomechanical FEM model of a typical glass-glass BIPV module in a ventilated façade was created as an example, based on an FEM model of conventional PV modules [3–6]. Each glass sheet has a thickness of 4 mm and a silicone casting resin is used as the cell encapsulation. The PV module has four strings of eight solar cells, each with dimensions of 156.75×156.75×0.18 mm³, and a PV module area of 1.2×0.6 m². A square hollow profile frame is attached adhesively to the back surface of the PV module, near its perimeter. Please note that the frame does not enclose the edge of the glass, as is the case with conventional PV module frames. A thermal FEM simulation determines the inhomogeneous temperature distribution inside the BIPV module due to partial shading for different shading geometries and ambient conditions (outdoor temperature and irradiation). Further thermal effects, such as hotspot formation, are not taken into account. We consider thermal radiation and convection as well as absorption within the single layers. To simplify the calculation, it was assumed that the solar reflectance was zero. For the ambient conditions, real and simulated weather data over 11 years are used. Particularly critical data sets are considered, which were identified in advance in another work package within the research project [2]. The coupled mechanical FEM simulation determines the thermally induced mechanical stress. The temperature $T$ and the first principal stress $\sigma_{\mathrm{I}}$ (tensile stress) in the front glass cover are evaluated in each case. The values in the back glass pane are only slightly different to those in the front glass cover. As an example for assessment criteria, the simulated stress is compared with the typical design edge resistances of 13.1 MPa and 75 MPa, as determined by Schwind *et al*. for annealed and thermally toughened glass, respectively [7]. If the simulated stress at the edge exceeds this limit, the design is assessed to be at risk of breakage.

The thermal model was successfully validated on full-size modules in a climatic chamber with a solar simulator. For this purpose, fully and partially covered PV modules were equipped with thermocouples at five positions over the module area of one PV module, as indicated in Figure 1, whereby two thermocouples were mounted at each such position, one on the back surface of the solar cell and one on the back surface of the back glass pane. Two such PV modules were mounted above each other, so that a total of ten thermocouple positions were investigated. The FEM model was adapted to the exact conditions of the experimental setup. The PV modules are mounted using conventional PV module clamps in front of a wooden panel, which represents the front of the façade. The climate chamber is set to a constant temperature of +10 °C. The irradiation varies between 900 W/m² to 1000 W/m² with a mean value of 920 W/m², which is the value used in the FEM simulation. Combined heat transfer coefficients, which are adapted to the measured temperature and wind speed are used. Due to the temperature inhomogeneity of the climate chamber, different values are used, as documented in Table 1. For each PV module design, a measurement sequence covering four different scenarios is performed, preceded by a stabilizing sequence:

1. Unshaded at maximum power point (MPP)
2. Unshaded under open circuit conditions (OC)
3. Horizontally shaded (using a metal sheet) in OC

Vertically shaded (using a metal sheet) in OC

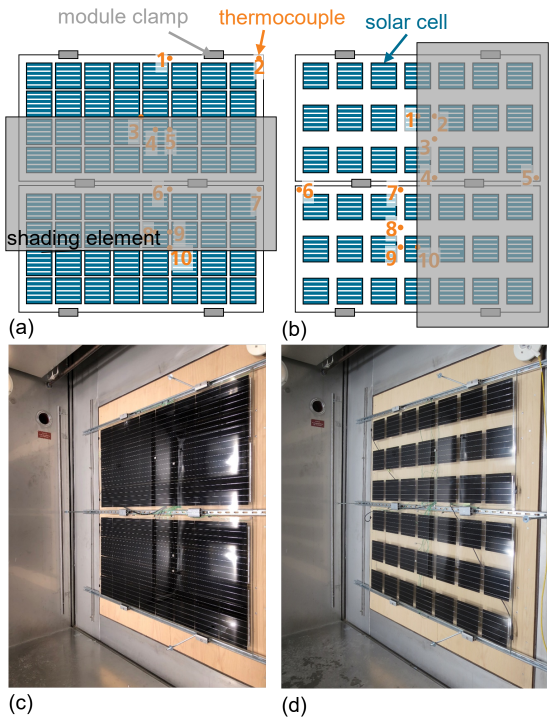


**Figure 1**: Schematic configuration of the PV modules used for experimental validation with (a) complete cell coverage and a horizontal shading element and (b) partial cell coverage and a vertical shading element. The orange numbers indicate the lateral positions of the thermocouples. For better visibility, the shading elements are illustrated semi-transparently. Corresponding experimental setup in the climate chamber with the PV modules with (c) complete and (d) partial cell coverage, without shading elements.

**Table 1**: Measured temperature and wind speed, as well as the corresponding calculated heat transfer coefficients calculated according to EN ISO 6946 for the upper and lower PV modules.

| | Temperature [°C] | Wind speed [m/s] | Heat transfer coefficients [W/(m²K)] | | |
|---|---|---|---|---|---|
| | | | Irradiation | Convection | Combined |
| **Upper PV module** | | | | | |
| **Front** | 11 | 4 | 4.7 | 20 | 24.7 |
| **Back** | 12.7 | 2 | 4.8 | 12 | 16.8 |
| **Lower PV module** | | | | | |
| **Front** | 13.2 | 2 | 4.8 | 12 | 16.8 |
| **back** | 15.6 | 0.2 | 4.9 | 4.8 | 9.7 |

Applying the validated FEM model, a sensitivity study is performed to investigate the influence of the following parameters:

1. Environmental conditions (irradiance and temperature, depending on orientation and location).
2. Frame
3. Operating conditions (MPP and OC)
4. Solar cell coverage
5. Edge distance from the cells to the glass edge
6. Glass thickness
7. Shading configuration
8. Crystalline silicon compared to thin film technology

Unless otherwise stated, all variations were carried out for the temporal profile of irradiation and temperature for a representative cold day shown in Figure 2, since higher stresses occur here than on a warm day (see 3.1 Environmental conditions).

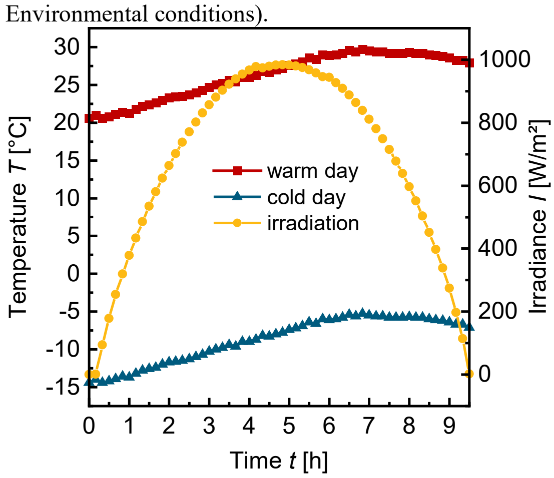


**Figure 2**: time course of temperature (left axis) of a representative warm (red squares) and cold day (blue triangles) as well as irradiance (yellow circles).

The results of the parameter sensitivity study were used to derive a simplified 2D FEM model, requiring less computational capacity. The 2D FEM model can be used for a standardized calculation procedure, for example in the planning phase of a BIPV façade. The approach "Determination of thermomechanical resistance to partial shading" was proposed for discussion by the standardization committee responsible for revising EN 50583:2016.

## 3 VALIDATION

Due to the page limitation, we present the results from only two representative sensor positions of the fully covered PV module in Figure 3. The full validation data can be found in the project report [2]. Except for the initial heating up, which was modelled in the FEM simulation with a pre-study, the simulation matches the experimental temperature curve well. Under maximum power point conditions and no shading, the deviation between FEM simulation and experiment is negligible. In open circuit without shading, the FEM simulation slightly overestimates the temperature of the experimental result by <1 K. In the case of shading and the OC state, the deviation becomes much larger, up to 5 K, with the FEM simulation resulting in lower temperatures. We suspect that the semi-shaded area around the metal sheet edges was not modelled correctly in the FEM simulation. Here a fading out of the shade was assumed. However, the unshaded temperature is simulated with good agreement to the measurements. Therefore, the thermal FEM model has been successfully validated.

## 4 PARAMETER VARIATIONS

### 4.1 Environmental conditions

In order to identify critical environmental conditions, a number of different conditions for different sky orientations were investigated in advance in a separate working package. As an example, Figure 4 shows the

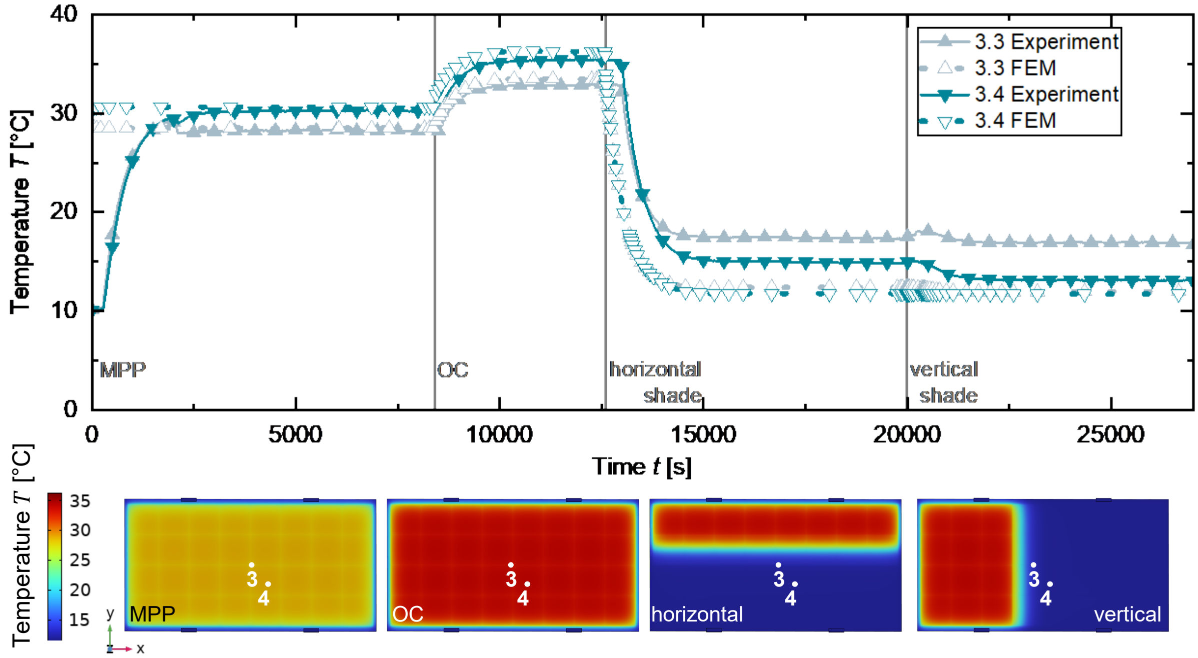


**Figure 3**: Experimental (closed symbols) and simulated (open symbols) temperatures $T$ of two selected positions on the back surface of a solar cell of the upper fully covered PV module. The 2D color plots show the complete temperature distribution over the module area at the end of each sequence.

temperature distribution and resulting mechanical stress for a warm day with temperatures between +20 °C and +30 °C and a cold day with temperatures between -10 °C and +5 °C (Figure 2) for homogeneously illuminated PV modules. The maximum irradiance is 1000 W/m² in each case and the modules are oriented to the south.

The temperature difference of 38 K between maximum and minimum temperature is 2 K greater on the cold day than on the warm day, which is also reflected in the slightly higher maximum stress in the front glass cover of 18.3 MPa (Figure 4). On both days, the maximum stresses exceed the design edge resistance of annealed glass, which means that even under homogeneous irradiation, the use of annealed glass must be considered to be risky. On the other hand, the maximum stresses are significantly below the design edge resistance of thermally toughened glass and are therefore not critical.

In summary, cold days with high irradiance levels were identified as the most critical environmental conditions. Consequently, all further investigations were carried out for these conditions.

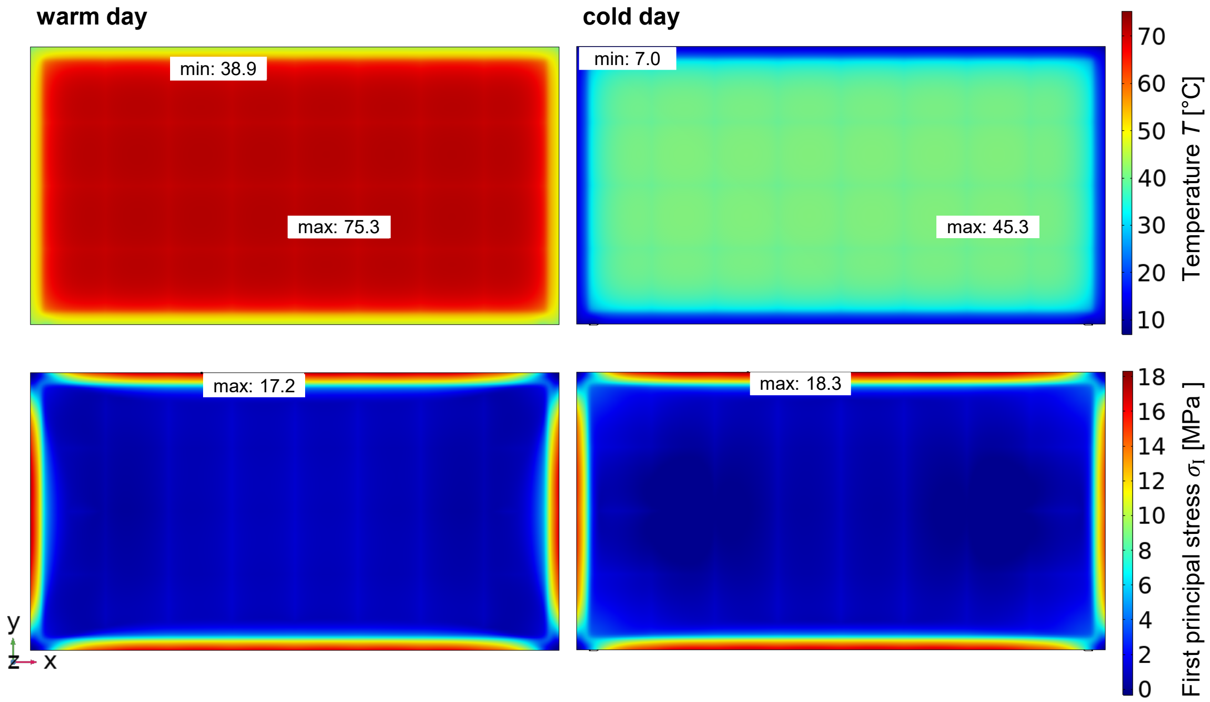


**Figure 4**: Temperature (top) and resulting stress (bottom) in the front glass cover of a homogeneously illuminated (up to 1000 W/m²) photovoltaic module on a warm (left) and cold day (right).

4.2 Frame

Three variants were simulated to investigate the influence of the module frame:

1. with frame and with absorption in the adhesive
2. with frame and without absorption in the adhesive
3. without frame

Figure 5 shows the resulting temperature distribution in the module cross-section at the position of the frame and the associated maximum first principal stress (tensile stress).

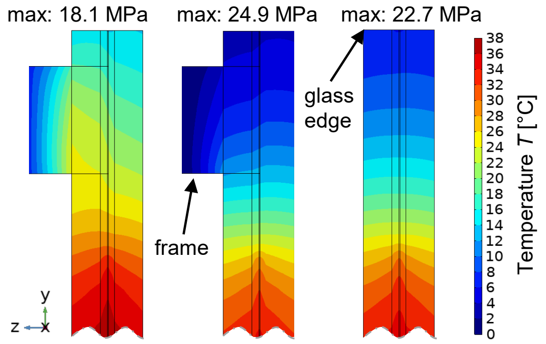


**Figure 5**: Temperature distribution in the module cross-section at the position of the frame for simulations with frame and absorption in the adhesive joint (left), with frame without absorption in the adhesive joint (center) and without frame (right). The resulting maximum stress at the edge of the glass is specified above the plots.

It can be seen that the frame has a significant influence on the temperature and thus the stress. On the one hand, the high absorption in the adhesive bond causes the module and frame to heat up, which is why a higher edge temperature occurs in the simulation with frame and absorption in the adhesive. On the other hand, the good heat conduction of the aluminum frame contributes to better heat dissipation to the environment, which in turn leads to a lower edge temperature compared to a frameless module. Accordingly, the frameless module's stress level is between that of the framed modules with and without absorption in the adhesive joint. All stresses at the glass edge exceed the design edge resistance of annealed glass, which is why annealed glass is to be considered risky. However, the stress is significantly below the design edge resistance of thermally toughened glass and hence is non-critical in this case. High absorption by the adhesive is advantageous, in order to reduce the mechanical stresses in the glass. This can be achieved, for example, by black adhesives.

4.3 Operating conditions

To investigate the influence of the operating conditions, the absorptance of the solar cell is adjusted. For the open circuit voltage, it is assumed that the incident radiation (after absorption by the glass and encapsulant) is absorbed completely by the solar cells. In the case of the maximum operating point, the absorptance is reduced by the solar cell efficiency of 22 %, resulting in a solar cell absorptance of 73 %. 5 % of the radiation is absorbed by the front glass cover and encapsulant. Figure 6 shows that the lower absorptance of the solar cell at the MPP leads to an approx. 10 K lower temperature in the area of the solar cells, while the temperature at the edge of the module remains almost unchanged. This results in an approx. 4.5 MPa lower stress in the glass. In the MPP state, the maximum stress at the edge of the glass corresponds to the design edge resistance of annealed glass, so that in both operating conditions annealed glass is considered risky, while thermally toughened glass is not.

In summary, OC operation is the more critical operating condition than MPP.

4.4 Solar cell coverage

We investigate three different cell coverages:

1. Fully covered: 4×8 solar cells
2. Partially covered: 3×7 solar cells
3. Lightly covered: 2×6 solar cells

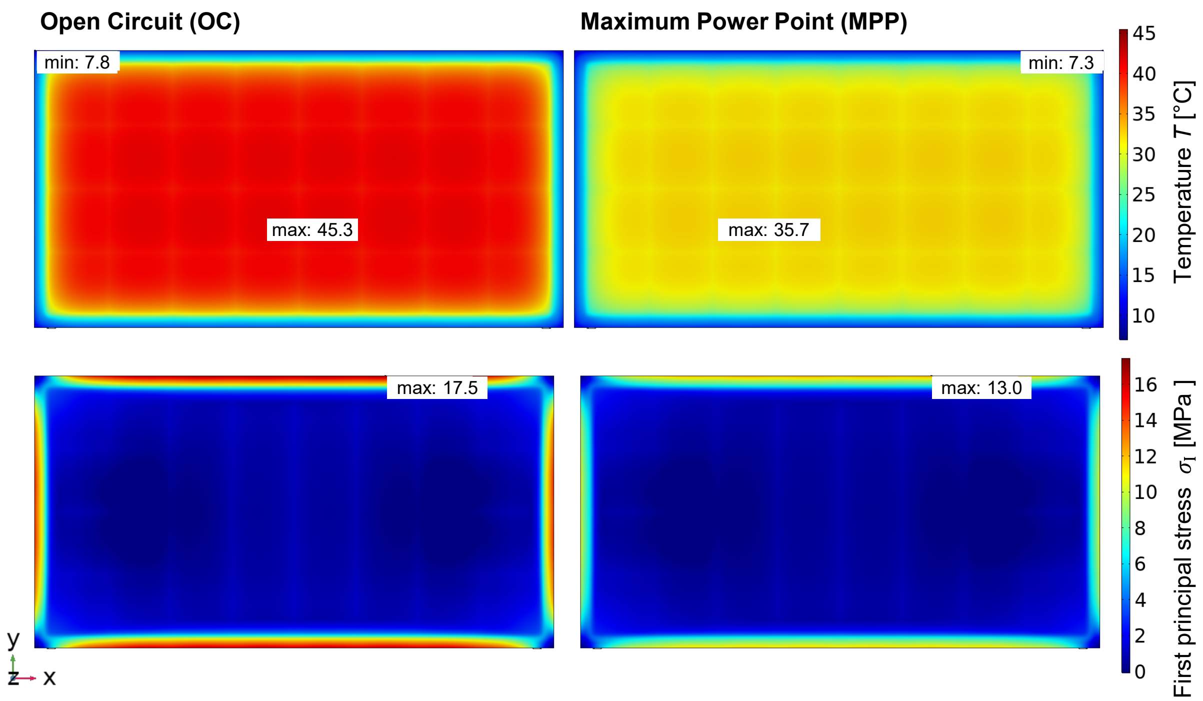


**Figure 6**: Temperature (top) and resulting stress (bottom) each in the front glass cover in the open-circuit (left) and maximum operating point (right) states.

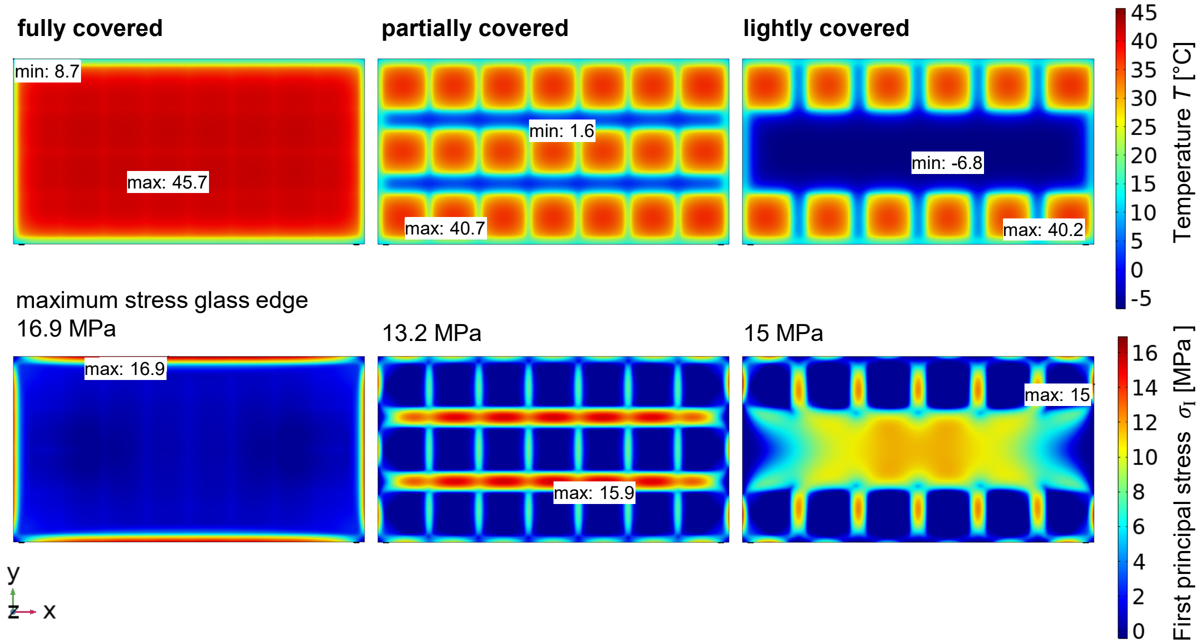


**Figure 7**: Temperature (top) and resulting stress (bottom) in each case in the front glass cover for fully covered (left), partially covered (middle) and lightly covered (right) PV modules with homogeneous irradiation. In addition to the maximum values, the maximum stress at the edge of the glass is indicated

Figure 7 shows the simulated temperature and mechanical stress. Due to the stronger heat generation, the fully covered PV module shows the highest maximum temperature of 45.8 °C. The difference between partially and lightly covered is not significant, with maximum temperatures of 40.7 °C and 40.2 °C, respectively. This shows that even a slight increase in cell spacing can reduce the temperature of the solar cell by up to 5 K. The coverage ratio has a much stronger effect on the minimum temperature, which drops from 8.7 °C with full coverage to -6.8 °C with light coverage. This significantly increases the temperature difference from 37 K to 47 K. However, the temperature gradient is weakened by lighter coverage, which is why the highest maximum stress of 16.9 MPa occurs in fully covered modules. Moreover, this occurs at the glass edge, which typically has the lowest fracture stress, whereas for partial coverage, the maximum stress at the glass edge is only 13.2 MPa, and is 15 MPa for light coverage. All coverage ratios lead to stresses that exceed the design edge resistance of annealed glass, which is why the use of annealed glass should be considered risky. However, they are well below the edge design resistance of thermally toughened glass and should be considered non-critical here.

In summary, fully covered PV modules are slightly more susceptible to thermally induced stresses.

4.5 Edge distance from the cells to the glass edge

We investigate two different perimeter width: a normal edge distance (long side: 28.8 mm, short side: 18.8 mm) and a very large edge distance (long side: 108.9 mm, short side: 99.9 mm). Figure 9 shows that the maximum temperature does not change significantly, while the minimum temperature drops from 8.7 °C to 2 °C with a large edge distance. Thus, the temperature difference increases from 37 K to 47.6 K. The resulting maximum stress increases from 16.9 MPa to 20.6 MPa, with the maximum stress at the edge of the glass being 17.5 MPa, which is only slightly higher but still above the design edge resistance of annealed glass, which is why the use of annealed glass must be considered risky. However, the design edge resistance of thermally toughened glass is significantly higher, so both edge distances can be rated as non-critical for thermally toughened glass.

In summary, the edge distance has a minor influence on thermally induced stresses.

4.6 Glass thickness

We vary glass thickness in 2 mm steps between 2 mm and 10 mm. The front and back glass panes have the same thickness. Figure 8 shows that the glass thickness has only a slight influence on the maximum stress in the glass. For 10 mm glass, the stress is reduced by 0.6 MPa compared to 2 mm. Due to the larger thermal mass, the time of maximum stress is shifted by about half an hour. Consequently, a greater glass thickness does not provide a significant advantage in reducing thermally induced stresses.

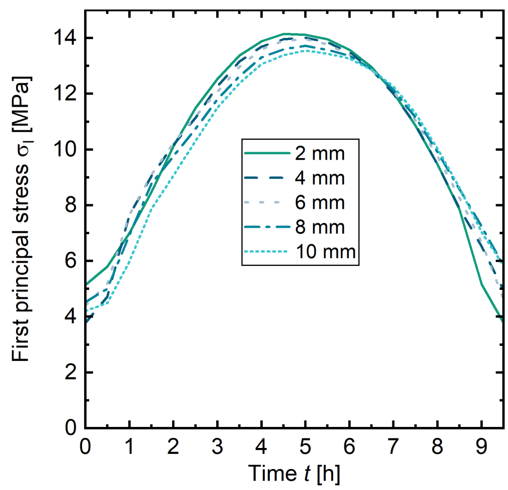


**Figure 8**: First principal stress in the glass over the course of the day for different glass thicknesses.

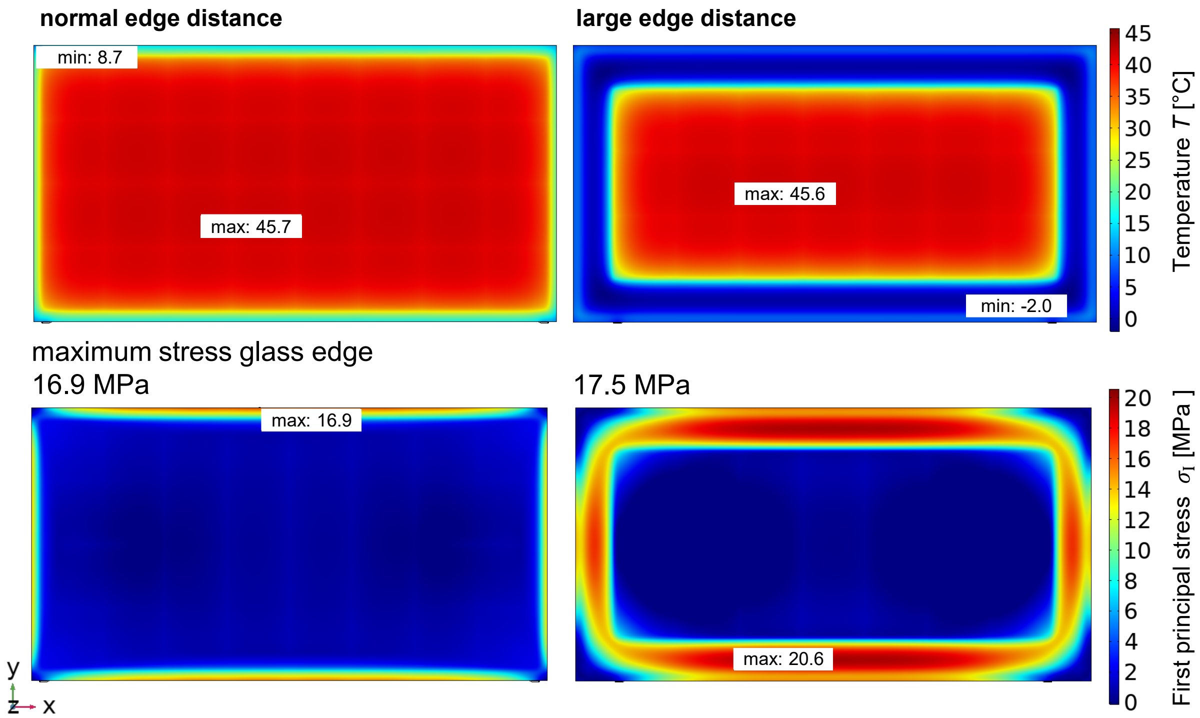


**Figure 9**: Temperature (top) and resulting mechanical stress (bottom) in the front glass for normal (left) and large (right) edge distance. In addition to the maximum values, the maximum stress at the edge of the glass is indicated.

4.7 Shading

Firstly, horizontal and vertical shading with 5 %, 10 % and 50 % degrees of shading with respect to the modules width or length were investigated. The simulated temperatures are shown in Figure 10. The maximum temperature decreases only at 50 % horizontal shading from 45.3 °C to 44.6 °C. The minimum temperature, however, is strongly dependent on the shadow width and ranges from -0.6 °C for 5 % horizontal shading to -8.0 °C for 50 % vertical shading. The resulting stress is shown in Figure 11. All shadows lead to significantly higher maximum stresses compared to unshaded PV modules, which all occur at the edge of the glass. The values range from 21.1 MPa (10 % horizontal and 5 % vertical) to 25.3 MPa (50 % vertical). There is no clear correlation between the surface area of the shadow and stress.

Secondly, a double diagonal shadow was considered. This starts in the middle of both long edges of the module and has its vertex at the middle of the short edge of the module. According to the "Guide for the Design, Construction and Control of Buildings with Structural Glass Elements" CNR-DT 210/2013 [8], this shading geometry is considered as "most dangerous" for structural glass elements. Figure 12 shows the simulated temperature and resulting stress. The maximum temperature is 45.3 °C, with -7.4 °C as the minimum temperature. Due to the very large temperature gradient at the top of the shadow, the highest maximum stress of 32.4 MPa is reached here. Compared with the unshaded PV module, the stress is almost twice as high, hence such shadows significantly influence thermally induced stress. For annealed glass in particular, the maximum stress is almost three times as high as the design edge resistance, which is why the use of annealed glass is assessed as being very risky. For fully toughened glass, the design edge resistance is more than twice as high as the maximum stress, so the risk of glass breakage purely due to thermal stresses is assessed as low. In a real installation case, however, thermally induced

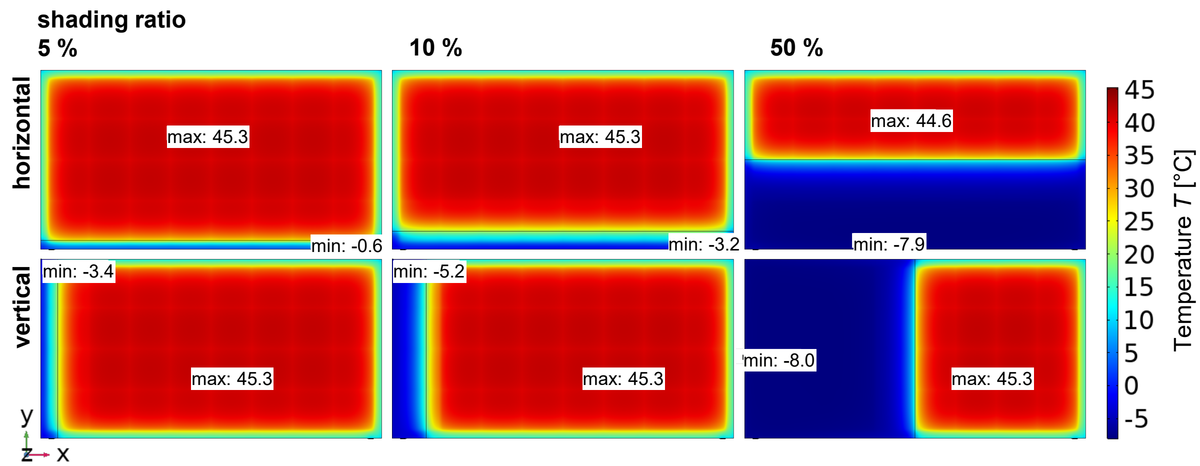


**Figure 10**: Temperature in the front glass cover for different shading configurations: top: horizontal shading; bottom: vertical shading, each with different shading ratios: 5 % (left) 10 % (center) and 50 % (right).

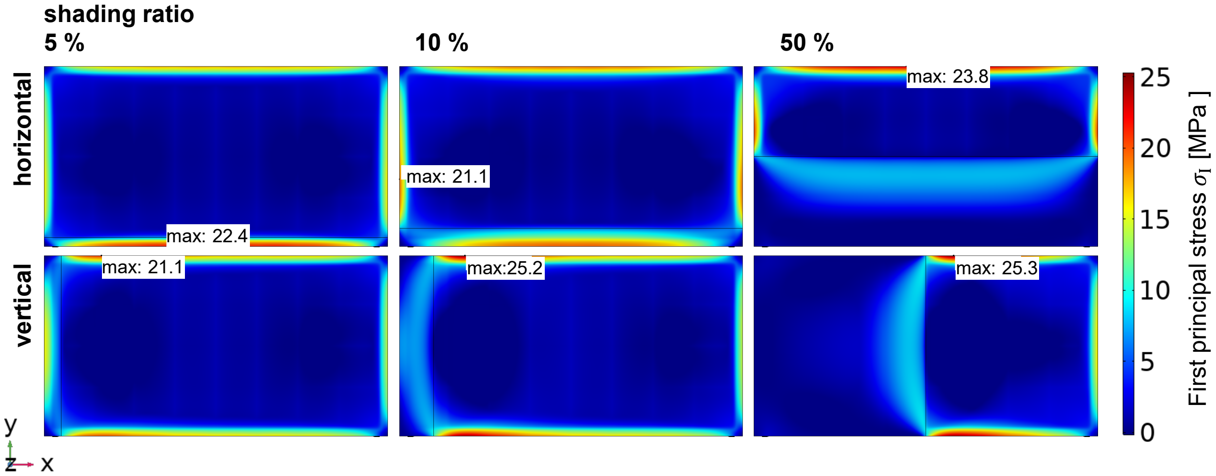


**Figure 11**: First principal stress in the front glass cover for different shading orientations and ratios: top: horizontal shading; bottom: vertical shading, each with different shading ratios: 5 % (left), 10 % (center) and 50 % (right).

stress is often superimposed with mechanically induced stress. This can result, for example, from wind load, snow load, self-weight or unplanned installation errors. It can be assumed that wind has a reducing effect on the thermally induced stress due to the increased convection and the associated cooling effect. With snow, on the other hand, a distinction must be made between full and partial coverage. In the case of full coverage, no stresses are caused by the shading and only the mechanical loads have an effect. In the case of partial coverage, the snow causes shading (and at the same time cooling of the module), which is why the thermally induced stress is superimposed on the snow load. Likewise, stress due to self-weight (with glass edges under tensile stress) and possible assembly errors in combination with thermally induced stress can lead to glass breakage.

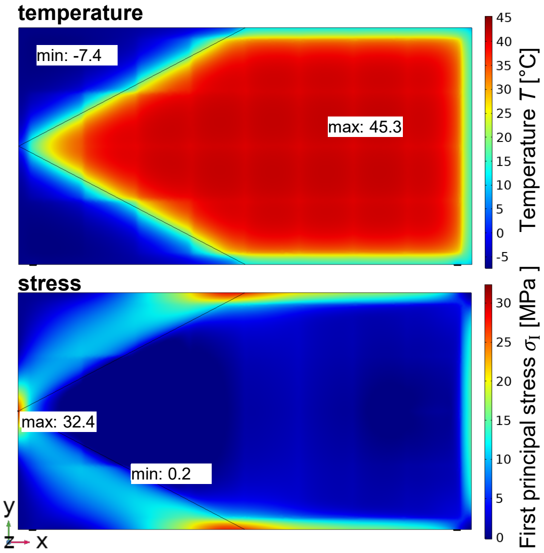


**Figure 12**: Temperature (top) and resulting first principal stress (bottom) in the front glass cover for a double diagonal shadow.

4.8 Difference between crystalline silicon and thin film cell technology

For the simulation of a thin film PV module, the solar cells were removed and replaced by an absorber layer positioned on the surface of the front glass cover facing away from the sun. Since the simulation was performed for the OC state, the different efficiencies did not have any influence. To simplify the calculation, it was assumed that the solar absorptance of both technologies is equal, which might not be the case depending on the thin film technology.

Figure 13 shows that due to the smaller absorber layer thickness and thus lower thermal mass, the maximum temperature in the thin-film module is almost 1 K lower. However, since the edge temperature is also slightly lower and the gradient from maximum to minimum temperature is larger, the thin-film module has a 1.5 MPa higher maximum stress. Consequently, the simulated thin film technology is slightly more susceptible to thermally induced glass breakage. However, it should be noted that thin-film modules generally use only annealed glass as the back glass, even when they contain drilled holes for cabling. This is risky because the design edge resistance of annealed glass is exceeded. By contrast, crystalline modules usually use thermally toughened glass with a higher design edge resistance that is not exceeded, and therefore is not critical.

5 SIMPLIFIED FEM MODEL

For the development of a standardized method, the 3D FEM model was simplified, in order to save computational cost and enable broad application. For this purpose, the combination with the greatest influence on thermally induced stresses was selected from the parameters investigated above. This resulted in a frameless, partially covered PV module with a double diagonal shadow, which is shown schematically in Figure 14. As a simplification, a 2D approach was chosen. The basic idea is to represent the PV module as a glass pane with the total thickness of the PV module. The glass pane has the material properties of the glass used, with adjusted absorptance coefficients at the positions of the solar cells and in the shaded area. These are shown in Figure 14. In addition, combined effective heat transfer coefficients are used: 10.5 W/(m²K) for the main module surfaces and 4 W/(m²K) for the edges. A constant 10 °C is chosen as the outdoor temperature. The same simplified boundary conditions are used in the 3D FEM model for comparison. Mechanically, the module is fixed at one corner point and a sliding bearing is attached to the neighboring corner point along the long edge.

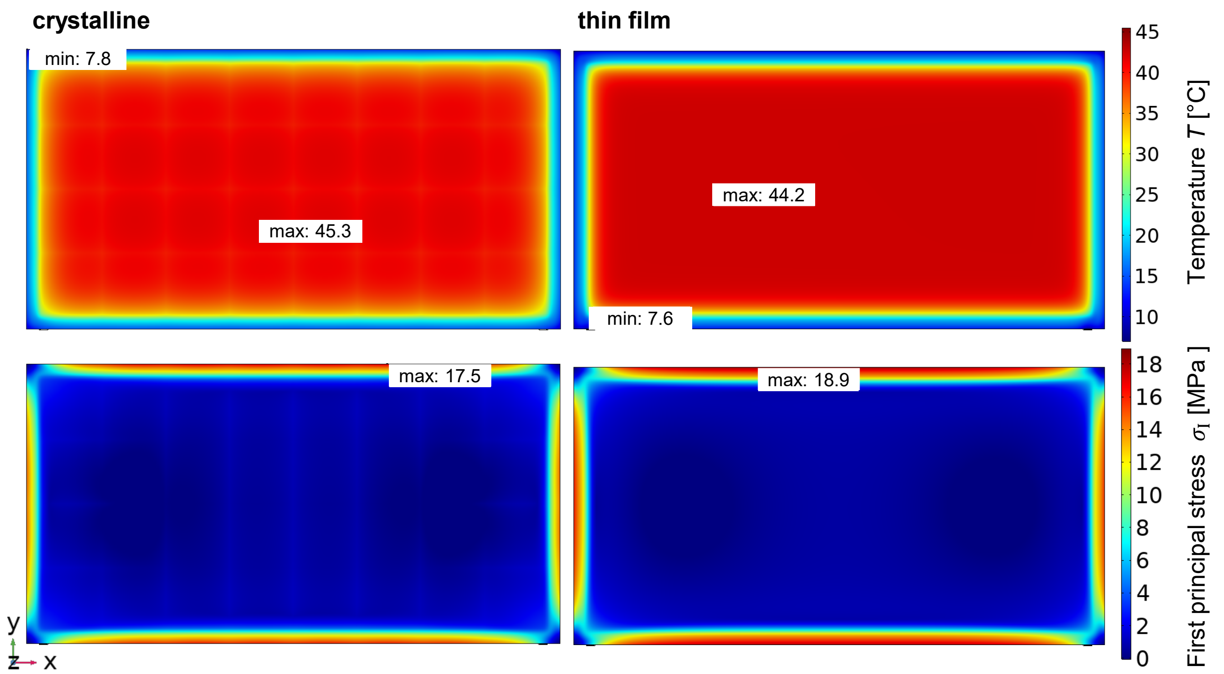


**Figure 13**: Temperature (top) and resulting mechanical stress (bottom) in the front glass cover for a crystalline PV module (left) and a thin-film PV module (right).

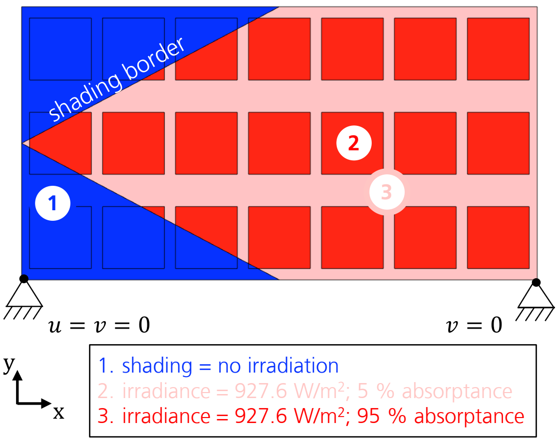


**Figure 14**: Schematic sketch of the simplified FEM model with division into the different absorptance and irradiance zones as well as the mechanical boundary conditions.

Figure 15 compares the simulation results for the temperature and Figure 16 the resulting mechanical stresses of the 2D simulation and the 3D simulation. Since in the 2D simulation the heat is homogeneously generated in the highly absorbing glass body itself, instead of being conducted from the solar cells to the glass, there is no temperature gradient between the absorbing solar cell and the glass surface. Hence, this leads to a higher temperature level compared to the 3D simulation. In particular, the maximum temperature of 46.5 °C is 5.1 K higher. However, the qualitative temperature distribution agrees well. For stress, the qualitative distribution also agrees very well and the higher temperature level leads to higher stress. The 2D FEM model has a stress of 34.7 MPa, which is 5.5 MPa higher than the 3D FEM model. Thus, the simplified FEM model offers the possibility to quickly estimate thermally induced mechanical stresses.

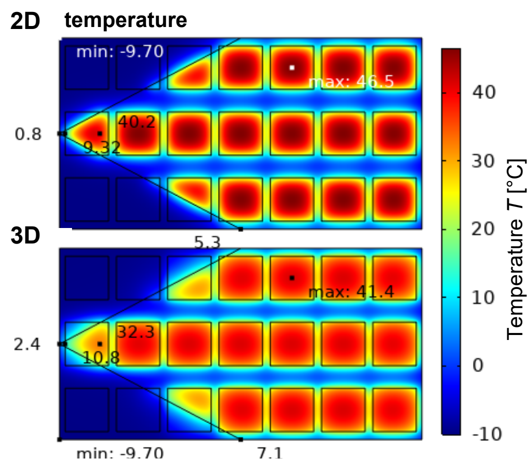


**Figure 15**: Comparison of temperature simulated with the simplified 2D model (top) and with the full 3D model (bottom). Values at characteristic points are marked.

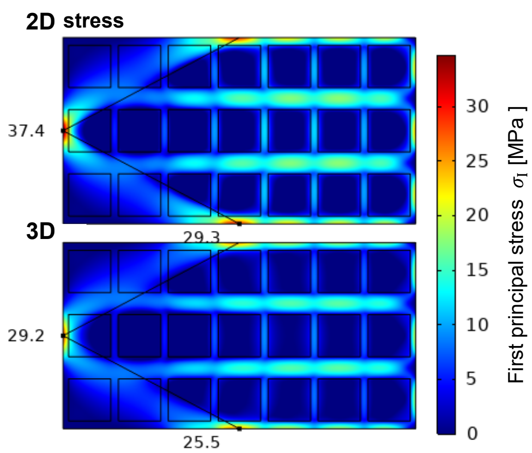


**Figure 16**: Comparison of stress simulated with the simplified 2D model (top) and with the full 3D model (bottom). Values at characteristic points are marked.

## 6 CONCLUSION

Both a very detailed thermomechanical 3D FEM model of a glass-glass BIPV module in a ventilated façade and a simplified 2D FEM model were developed. The 3D thermal model was successfully validated, displaying good agreement with the experimental data. The performed parameter variations have shown that even for homogeneous irradiation, the glass stress can exceed the design limits for annealed glass edges. Partial shading can lead to a significant increase of the stress and should therefore be considered in the design of a PV system, especially if thermally toughened glass is not used. Overall, for the simulated glass-glass BIPV module, all variations resulted in maximum stresses exceeding the reference design edge resistance of annealed glass determined by Schwind *et al*. [7]. Consequently, the use of annealed glass must be considered to be risky. Also, the use of thin glass, which can only be partly thermally toughened, may become risky. However, the edge resistance of fully thermally toughened glass was not exceeded in any variation, so the use of fully thermally toughened is rated as being non-critical. The other results are:

1. During the course of a year, cold days with high irradiation induce the highest stresses.
2. Open Circuit (OC) conditions induce higher stress than maximum power point (MPP).
3. Shading has a significant impact on the stress. In particular, a double diagonal shadow shape can double the stress.
4. Fully covered PV modules have slightly higher mechanical stress than partially covered ones.
5. The edge distance from solar cell to glass edge has a very small effect on the maximum stress at the glass edge.
6. The glass thickness has a minimal influence.
7. Thin-film PV modules have a slightly higher stress than crystalline silicon PV modules.
8. A frame adhesive with high absorption reduces stress in the glass.

## 7 ACKNOWLEDGEMENTS

The authors would like to thank Markus Heck for the careful planning and execution of the validation experiments at Fraunhofer ISE. Also, the authors would like to thank the German Federal Ministry for Economic Affairs and Climate Action for the financial support within the project: “Thermobruch” (03TN0007C).

## 8 REFERENCES

[1] F. Ensslen, G. Schwind, J. Schneider, A. Beinert, A. Mahfoudi*, et al.*, Challenging Glass Conference Proceedings (2022), 10.47982/cgc.8.433.

[2] F. Ensslen, A.J. Beinert, A. Mahfoudi, W. Herzberg, E. Lorenz*, et al.*, Normentwurf zur Ermittlung der thermischen Beanspruchung von Glas und Glas-PV-Modulen (BIPV) im Bauwesen (Thermobruch) - Schlussbericht zum WIPANO-Projekt (FKZ: 03TN0007A-D), (2023).

[3] A.J. Beinert, P. Romer, M. Heinrich, J. Aktaa, D.H. Neuhaus, Prog. Photovoltaics Res. Appl. (Progress in Photovoltaics: Research and Applications), (2022), 1–13, 10.1002/pip.3624.

[4] A.J. Beinert, P. Romer, M. Heinrich, M. Mittag, J. Aktaa*, et al.*, IEEE J. Photovoltaics 10, (2020), 70–77, 10.1109/JPHOTOV.2019.2949875.

[5] P. Romer, K.B. Pethani, A.J. Beinert, 8th World Conference on Photovoltaic Energy Conversion: Joint Conference of 39th European Photovoltaic Solar Energy Conference and Exhibition, 50th IEEE Photovoltaic Specialists Conference, 32th International PV Science and Engineering Conference. Conference Record (2022), 924–929, 10.4229/WCPEC-82022-3DV.3.27.

[6] P. Romer, A.J. Beinert, Proceedings of the 38th European Photovoltaic Solar Energy Conference and Exhibition (EU PVSEC) (2021), 602–606, 10.4229/EUPVSEC20212021-4BO.4.5.

[7] G. Schwind, F. Paschke, J. Schneider, Challenging Glass Conference Proceedings – Volume 8 (2022), 1–37, 10.47982/cgc.8.388.

[8] National Research Council of Italy – Advisory Committee on Technical Recommendations for Construction CNR-DT 210/2013, Guide for the Design, Construction and Control of Buildings with Structural Glass Elements (2013).